Available online at http://scik.org
Commun. Math. Biol. Neurosci. 2024, 2024:115
https://doi.org/10.28919/cmbn/8843
ISSN: 2052-2541

DISCOVERING THE IMPORTANT PROTEINS THROUGH PERSISTENT HOMOLOGY IN AGING PROTEIN-PROTEIN INTERACTION NETWORKS

ABDUL SYUKOR HAZRAM, SAKHINAH ABU BAKAR*, FATIMAH ABDUL RAZAK

Department of Mathematical Sciences, Faculty of Science and Technology, Universiti Kebangsaan Malaysia, Bangi, 43600, Malaysia

Abstract. A Protein-Protein Interaction Network (PPIN) is a mathematical model in which every protein is described as a node, and the physical interaction or similar protein expression is considered an edge. Previous studies have shown that PPIN performs various analyses and protein predictions in many aspects, such as essential protein prediction and drug targeting. Numerous centrality measures can provide protein characterization at the node level. However, we still have insufficient network-level identification. In this study, Persistent Homology (PH) is incorporated as an additional network-level measurement to analyze 42 aging PPINs, comprising 22 males and 20 females, aged between 20 and 99. The Vietoris-Rips (VR) filtration was used to capture simplicial complexes before obtaining the persistent barcodes, which are considered the topological representation of a network. The derivation of persistent barcodes, named the Betti Sequence, is calculated for each network, which represents the complexity of the network. Node deletion is performed to assess the change in complexity of the network. The findings reveal a significant change in the Betti sequence after node deletion, indicating that the node is crucial within the network and could potentially serve as a drug target.

Keywords: persistent homology; protein-protein interaction network; mathematical model.

2020 AMS Subject Classification: 05C82, 55N31.

*Corresponding author

E-mail address: sakhinah@ukm.edu.my

Received August 16, 2024

1. INTRODUCTION

Aging is a continuous process in every living organism. For humans, it usually begins in their early 20s. Previous research has demonstrated that aging manifests not only physically, such as in bone acidity formation [1], muscle architecture [2], and the immune system [3], but also mentally [4]. Proteins are believed to play a crucial role throughout the aging process [5], underscoring the importance of studying protein interactions to characterize their behaviors and ascertain their essential roles. Hence, characterizing essential proteins is important as they have various applications in the medical and pharmaceutical fields, such as drug targeting and design.

The study of essential proteins in aging can be conducted by either a biological laboratory (wet lab) or computational biology. There are numerous methods to characterize essential proteins, including machine learning [6] and network analysis [7, 8]. In this study, we employed a computational approach to construct human aging Protein-Protein interaction Interaction Networks (PPIN).

A network G can be defined as $G = (V,E)$; where V is the collection of nodes and E is the collection of edges. In PPIN, the nodes represent proteins whereas the edges are defined as the connections between any two proteins, usually sharing similar protein expressions or physical interactions. The measurements in a network can provide information regarding the importance of their connectivity. For example, proteins with high degree, closeness or betweenness values have a high tendency to become essential proteins [7]. Apart from the centralities, another measure used in aging PPIN is clustering [9]. It measures the tendency of nodes (proteins) to form a cluster by using the Local Clustering Coefficient (LCC) [7].

These classical graph-theoretic measures are beneficial for understanding the nodes and their interactions. However, they focus on the node level and do not account for the overall network topology. Therefore, they may have information loss over topological structures, such as the clique, connected components or holes in the networks. On the other hand, the structure of the holes in networks could provide important information about network topology [10]. For instance, node importance can be measured based on the structure of the holes by identifying the location of holes in which can reveal the new characteristics of the network, that can be used for network comparison and classification [11].

Recently, Persistent Homology (PH) has been widely applied to study complex networks as a topological feature extractor since PH provides a multi-scales summary of the network and differs from most the existing centralities that summarize the network from a specific point of view. Therefore, the objective of this study is to implement PH in analyzing aging PPIN of Homo Sapien. Furthermore, proteins are identified by examining topological changes following node perturbation. These identified proteins are subsequently analyzed based on network topology and their essentiality.

2. PERSISTENT HOMOLOGY FOR NETWORKS

Extracting information from complex or high-dimensional datasets is typically challenging. Thus, PH, one of the tools in Topological Data Analysis (TDA) may provide a general framework to analyze several data types, such as point-cloud data [12], image [13], time series [14], as well as network data. In this section, we are focusing on utilizing PH in network analysis. The notion of PH in analyzing data is illustrated as in Figure 1.

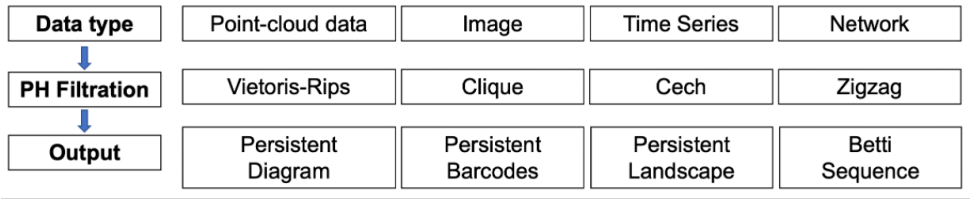

FIGURE 1. Flowchart illustrating the process of Persistent Homology.

The PH analysis can be divided into two main parts, which are the filtration process and feature selection. The filtration process is the process of extracting topological features in different spatial resolutions. In network analysis, the usual topological features involve 0-D and 1-D components, often referred to as connected components and loops within the network structure. The simplest 0-D components, known as simplices, serve as fundamental building blocks in constructing the simplicial complex. The example of 0-D topological components is illustrated in Figure 2:

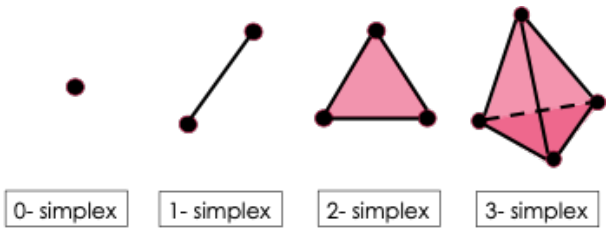

FIGURE 2. List of topological simplices.

There are various filtration processes available, each suited to different types of networks. One of the most commonly used filtrations for network analysis is the Vietoris-Rips (VR) filtration [15], known for its stability in most undirected network cases. Other filtration methods include Dowker Sink and Source (DSS) filtration [16], Clique Complex (CC) filtration [17], zigzag filtration [18], temporal filtration [19], Weighted Simplex (WS) filtration [20], power filtration [21], and Vertex-Based Clique (VBC) filtration [22]. Note that each filtration method serves a specific purpose in extracting topological features, making them suitable for particular types of networks. For example, temporal filtration is ideal for dynamic temporal networks, while zigzag filtration is specifically designed for dynamic networks. In this study, the network type under consideration is an undirected static network. Therefore, suitable filtrations include power filtration, VR filtration, WS filtration, and VBC filtration [15].

The next important process is choosing the right topological features for analysis to obtain the desired output. The basic output for PH analysis is barcodes. Other features derived from barcodes are Betti Number, Persistent Diagram (PD) and Persistent Landscape (PL). There are multiple ways to analyze the output, such as features comparison, data perturbation, or entropy [15]. Some of past applications of PH in static network are listed in Table 1.

Most studies primarily utilize VR filtration due to its accessibility and simplicity in capturing topological features for analysis in conjunction with PD for feature selection. Given that our network type is undirected, we sought to explore alternative filtration methods. Instead of using power filtration as in [21], we employed VR filtration and utilized Betti Sequences (a sequence of Betti Numbers) for feature selection, aiming to provide a more comprehensive understanding of the network's topological characteristics.

TABLE 1. Summary of PH filtration and topological features for analysis of different network types

Authors	Network Type	Filtration Used	Topological Features
Benzekry et al. [21]	PPIN	Power	Betti Numbers
Chung et al. [23]	Brain networks	Vietoris-Rips	Persistent Diagram
Giusti et al. [24]	Brain networks	Weighted Simplex	Persistent Diagram
Ignacio and Darcy [25]	Migration networks	Vietoris-Rips	Persistent Diagram
Khalid et al. [26]	Brain networks	Vietoris-Rips	Persistent Diagram
Rieck et al. [22]	Brain network	Vertex-based Clique	Persistent Diagram
Rucco et al. [27]	Simulated network	Vietoris-Rips	Barcodes
Sizemore et al. [28]	Brain network	Vietoris-Rips	Persistent Diagram
Suh et al. [29]	Co-occurrence network	Power	Barcodes

3. METHODOLOGY

The study comprised four primary stages: constructing the PPIN, obtaining the metric space representation of these PPINs, calculating PH from the metric space, and analyzing the Betti Number Sequence (BNS) derived from the PPINs.

3.1. Aging Protein-Protein Interaction Network of Homo Sapiens. The PPIN were built using aging proteins collected from four parts of the human brain: the Entorhinal Cortex (EC), Hippocampus (HC), Post-Central Gyrus (PCG) and Superior Frontal Gyrus (SFG) [30]. The protein samples were taken from 55 individuals and represented by the network nodes. Consequently, we referred to the Data of Interacting Proteins (DIP) to create the interactions between the proteins, which serve as the edges of the network [31].

As a result, a total of 42 different unweighted and undirected networks were constructed according to the age and gender of the individuals. The giant components of those networks were extracted for further analysis. A giant component is the largest connected component in a network. It is important to extract the largest connected components of the PPIN because smaller, disconnected components often consist of nonessential proteins [32].

3.2. Metric Space Representation of Aging PPIN. In this stage, all unweighted networks were converted into weighted networks. We defined the edge weight of these networks by using distance metrics. Originally, the two common methods to obtain weighted networks were the shortest path algorithm and the Laplacian method. Some of the well-known shortest path algorithms were conceived by Dijkstra, Johnson, Floyd-Warshall and Bellman-Ford. On the other hand, examples of Laplacian methods include the commute-time distance [33], biharmonic distance [34] and diffusion distance [35]. Here, we chose the Johnson algorithm from the shortest path algorithm because it has a low computational cost and suits the best with the nature of our networks – low density and sparse network [36].

3.3. Persistent Barcodes and Betti Number Sequence. Barcodes are the first PH features obtained after filtration. The filtration that we used in this study is VR filtration, defined as follows [15]:

Definition 1: Vietoris-Rips filtration. Let $G = (V,E)$ be an undirected graph with weight function $W : V \times V \to \mathbb{R}$ defined on E. For any $\delta \in \mathbb{R}$, the $G_\delta = (V_\delta, E_\delta) \subset G$ is defined on the subgraph of G where $V_\delta = V$ and its edge set $E_\delta \in E$ only include the edges whose weight is less than or equal to δ. Correspondingly, for any $\delta \in \mathbb{R}$, the Vietoris-Rips (VR) complex as the clique of the G_δ was defined as $Cl(G_\delta)$. The VR filtration is then defined as:

$$Cl(G_\delta) \hookrightarrow Cl(G_{\delta'})$$

In other words, this filtration begins with a set of vertices. The edge weights range from the minimum weight, w_{min} to the maximum weight w_{max}. At each step, edges are added according to their weights, and the simplicial complex of the threshold subgraph G_δ is constructed. This process differs slightly from the original filtration process used on point cloud data, as distances between nodes in this network context are defined by edge weights.

A combination of simplices that are connected is called a simplicial complex. Simplices and complexes can be seen when the filtration process is completed after a certain filtration threshold. Note that filtration determines the connection of the components in the data at specific spatial resolutions and is also represented by the distance between the points [37]. The records

on this process are visualized using barcodes, the length of which is defined by the lifetime of each topological components.

On the other hand, barcodes can measure the persistency of the topological features by returning the value of their births and deaths. The birth time represents the spatial resolution when the connected components, for 0-dimensional, or loops, for 1-dimensional, of a topological feature are formed, while the death time is when the components or loops diminish. The length of the barcodes is referred to as lifetime and is calculated by taking the difference between the death and birth of topological components. The example of a toy model and its barcode is illustrated in Figure 3.

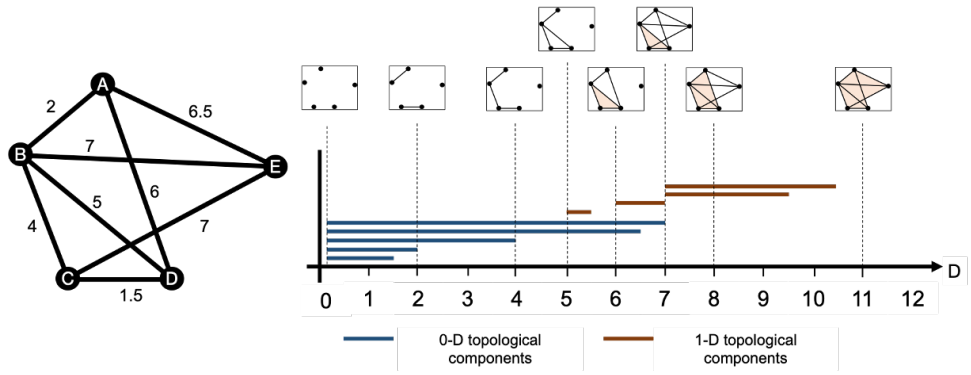

FIGURE 3. The toy model of the weighted network, along with the VR filtration process. The connection among the nodes of the network is shown at a certain spatial resolution, D. For example, when $D = 2$, the edge with weight 2 and less $\{$A,B$\}$ and $\{$C,D$\}$ are connected.

In Figure 3, notice that the number of lines for both 0-D and 1-D represents the number of topological components in respective dimensions. In addition, the lifetime of the longest barcode is finite. That highlighted the difference between filtration in a network and filtration for a point cloud data, which is the longest barcode persists from $[0,\infty)$ [35]. At different values of D, the number of bars is different, and it can represent a Betti number. In this paper, we specify the step size of $0.5D$ to obtain the number of topological components (total number of bars). The sequence of every topological component at the same step size is denoted by a BNS [38]. With the step size of $0.5D$, the BNS in which includes 0-D and 1-D topological

components from Figure 3 is:

$$\beta = \{5,5,4,3,3,3,3,2,2,3,2,3,3,3,3,3,3,3,2,2,1,1,0,\ldots\}$$

In a large network setting, it is possible that different network will produce different BNS. Hence, it may be considered as unique [15]. If there is a minor perturbation in the networks, BNS will also be affected. Moreover, there are several perturbation methods, involving adding or removing the nodes or edges [35]. We only focusing on single node deletion and observe how removing a node affects the topology of the network. Figure 4 demonstrate the flow chart of the network perturbation process.

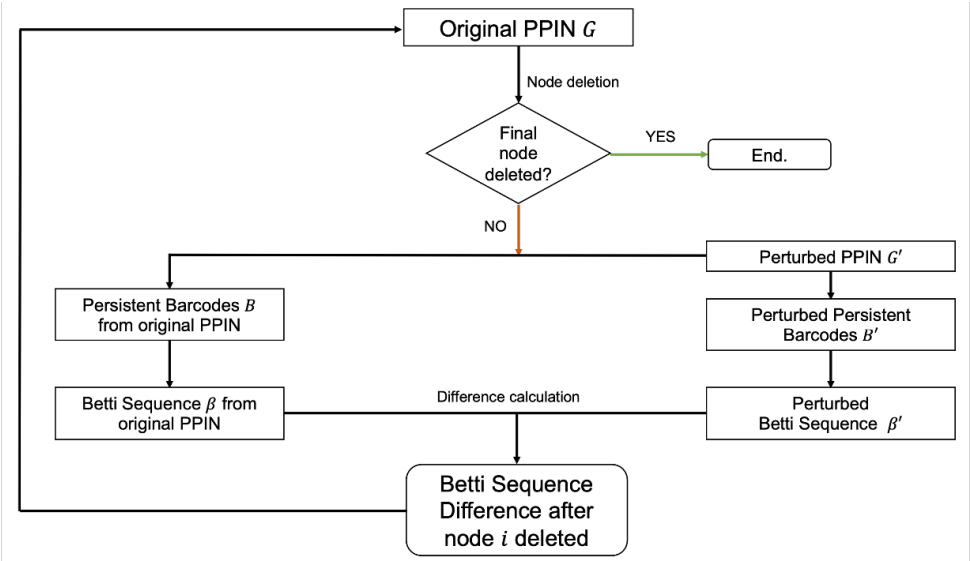

FIGURE 4. Flow chart of network perturbation.

The difference between original BNS and perturbed BNS is computed using the following formula:

$$D_{BNS} = \sqrt{\sum_{i=1}^{n}(x_i - y_i)^2}$$

such that x_i is the i-th Betti number in the sequence obtained from the original PPIN, y_i is the i-th Betti number in the sequence obtained from perturbed PPIN, and n is the length of the sequence.

4. RESULTS

This section will comprehensively discuss the results in two parts. The first part involves calculating the BNS at the network level. Subsequently, the difference between the BNS of the original network and the perturbed network will be discussed. In the second part, proteins exhibiting significant differences in BNS will be identified and their essentiality will be discussed.

4.1. Node Importance Using Perturbation. We have a total of 42 PPIN datasets, comprising 22 male PPINs and 20 female PPINs. For each network, nodes were deleted one at a time, and PH was computed to obtain the BNS of the perturbed PPIN. Since we have multiple static networks for each gender, certain proteins are expressed in some networks but not in others. Therefore, for each protein, the average BNS difference $\overline{D_{BNS}}$ is calculated based on the networks in which the protein is expressed.

On the other hand, we also calculate the network centrality to observe the node level measurements for each protein and also the relation of topological changes of the network after protein removal with the node level measures of proteins in the network. In this study, we selected six node-level measurements: Degree Centrality (DC), Closeness Centrality (CC), Betweenness Centrality (BC), Eigenvector Centrality (EC), Reach Centrality (RC), and LCC. The process of obtaining centrality values for each protein is analogous to $\overline{D_{BNS}}$, which represents the average centrality value based on the networks in which the protein is expressed and categorized by gender. Therefore, for each centrality comparison across networks, we will analyze outputs from both male and female aging PPINs.

As a result, proteins present in both male and female PPINs were identified, along with their average BNS difference and node-level measurements. For each gender, we extracted the top 10% of proteins exhibiting the largest BNS differences and compared them with the remaining 90% of proteins based on their centralities.

4.1.1. *Degree Centrality.* DC measures the number of proteins connected to a protein. A high DC value of protein results a high connection made from a protein to the others. The removal of proteins with high degree will significantly change the topology of the network. Hence, the BNS difference of perturbed network with respect to the original network is large. Figure 5

illustrates proteins with high degree centrality are placed among the top 10 percent that giving a high difference of BNS. The correlation of $r = 0.7367$ and $r = 0.7369$ for both male and female PPIN suggested that the deletion of proteins with high DC value will affect the network topology. Consequently, it produces a large difference of BNS.

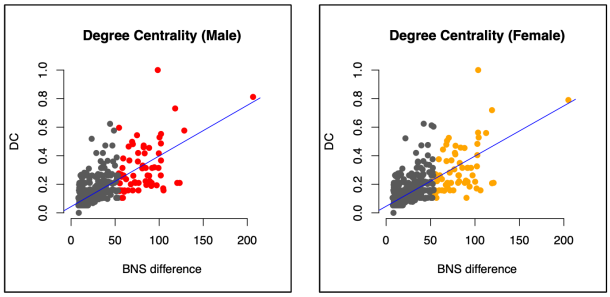

$r_{DC} = 0.7367$ $r_{DC} = 0.7369$

FIGURE 5. Graph of average BNS difference against average Degree Centrality for both male and female aging PPINs. The coloured markers represent the top 10% of highest average BNS difference.

4.1.2. *Closeness Centrality.* CC measures the distance from a protein to the other proteins via the shortest path. The overall range of CC for both male and female is low, in which $0.00026 \approx 0$. This means that most of the proteins are equidistant from one another. This also results a weak correlation between BNS where the values are $r = 0.3675$ and $r = 0.3740$ for males and females respectively, as illustrated in Figure 6. Since the values for each node centrality is relatively low, this measurement will be excluded for further analysis as it does not represent the characterization of the network.

4.1.3. *Betweenness Centrality.* Similar to CC, BC also measures the shortest path between any two proteins but focuses on the frequency of another protein being in the pathway of those two nodes. There are several of BC calculation formulae such as the original formulation from [39] or the extended version from [40]. For this study, we calculated the BC for each protein using [39]. Most proteins with high BC are also among the top 10% with significant BNS differences after node deletion. The rationale behind this is as follows.

- Proteins with high BC often serve as central nodes situated along pathways connecting multiple proteins.

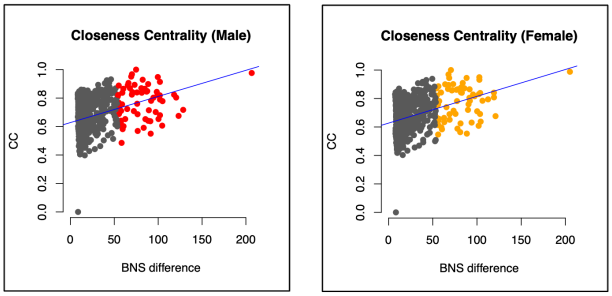

$r_{CC} = 0.3675$ $r_{CC} = 0.3740$

FIGURE 6. Graph of average BNS difference against average Closeness Centrality for both male and female aging PPINs. The coloured markers represent the top 10% of highest average BNS difference.

- Deleting proteins with high BC can split the network into disconnected components, substantially altering the overall network topology.

Moreover, Figure 7 demonstrate that the correlation between proteins' BC and BNS difference is the strongest among all six centralities, with correlation coefficients of $r = 0.8332$ for male PPIN and $r = 0.8459$ for female PPIN, indicating that high BNS differences are closely linked with BC.

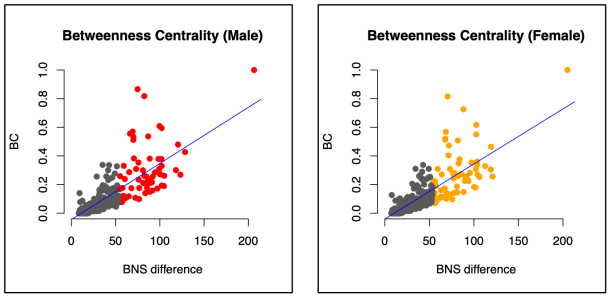

$r_{BC} = 0.8332$ $r_{BC} = 0.8459$

FIGURE 7. Graph of average BNS difference against average Betweenness Centrality for both male and female aging PPINs. The coloured markers represent the top 10% of the highest average BNS difference.

4.1.4. *Eigenvector Centrality.* The EC of a protein is the measure of the influence of a protein over the network. Proteins with high EC tends to be linked with proteins of high degree. Based on Figure 8, the correlation of average EC with average BNS difference is low, which are

$r = 0.1019$ and $r = 0.09713$ for male PPIN and female PPIN respectively. This also shows that the perturbation of proteins with high EC does not necessarily change the network topology. Certain proteins with high EC in the top 10% highest BNS group also exhibit high BC or DC.

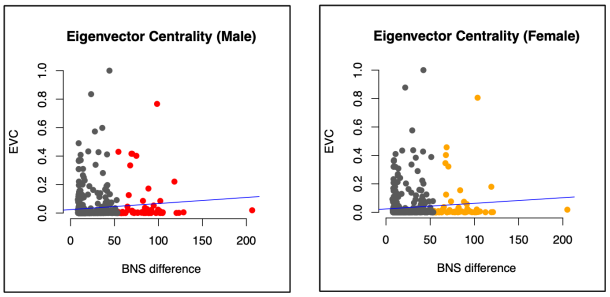

$r_{EC} = 0.1019$ $r_{EC} = 0.09713$

FIGURE 8. Graph of average BNS difference against average Eigenvector Centrality for both male and female aging PPINs. The coloured markers represent the top 10% of the highest average BNS difference.

4.1.5. *Reach Centrality.* RC is the extended version of DC. While DC calculate the number of adjacent proteins of a protein, RC calculate the number of proteins within up to nth degree (usually n up to 3.). Our study defines RC by calculating the number of neighboring nodes up to the third degree. A high RC value suggests that:

- The protein is centrally located within the network and has extensive connectivity.
- The protein is connected to other proteins with high degrees or is situated within neighborhoods containing proteins with high average DC.

Although DC has a strong correlation (> 0.7) with BNS difference, by extending the neighbors to the third degree reduces the correlation, which is $r = 0.5694$ and $r = 0.5656$ for both male and female PPIN, as depicted in Figure 9.

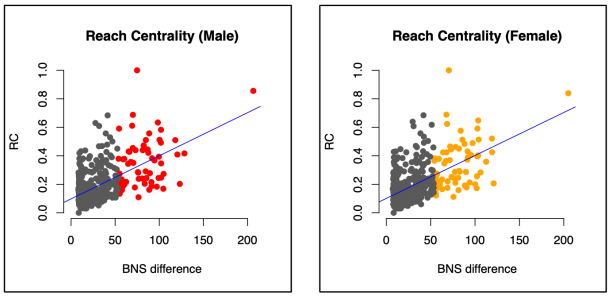

$r_{RC} = 0.5694$ $r_{RC} = 0.5656$

FIGURE 9. Graph of average BNS difference against average Reach Centrality for both male and female aging PPINs. The coloured markers represent the top 10% of the highest average BNS difference.

4.1.6. *Local Clustering Coefficient.* Extensive interconnections among proteins can fragment the network into multiple modules. Thus, LCC assesses the likelihood of proteins being grouped into these modules, while also measuring how closely a protein's neighbors resemble a clique. Figure 10 illustrates that proteins with high BNS differences tend to have low LCC values. The correlation coefficients, $r = -0.1585$ for male PPIN and $r = -0.1603$ for female PPIN, indicate a weak negative correlation, suggesting that LCC may not be suitable for characterizing proteins in further analysis.

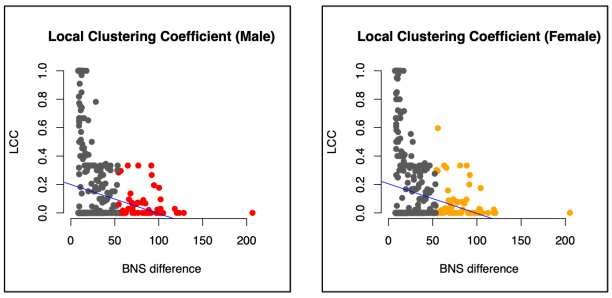

$r_{LCC} = -0.1585$ $r_{LCC} = -0.1603$

FIGURE 10. Graph of average BNS difference against average local clustering coefficient for both male and female aging PPINs. The coloured markers represent the top 10% of the highest average BNS difference.

5. DISCUSSION

5.1. Summary. Our approach aims to assess global topological changes following node removal. We compare the differences in BNS with various node-level centralities to gauge the significance of nodes in local connectivity. Only two of six network measurements show a strong positive correlation: DC and BC.

In these aging PPINs, important proteins in maintaining network topology tend to have high BC or DC. Rather than analyzing each PPIN separately for different centralities, PH combines these measures into a unified analysis. According to [21], BNS can indicate network complexity. Consistent with our findings, proteins contributing to higher topological changes often have high degrees or betweenness centrality. Table 2 illustrates a significant disparity between these two groups in average DC and BC values.

TABLE 2. Average Degree Centrality (DC) and Betweenness Centrality (BC) for Male and Female Proteins

Gender	Group	Average DC	Average BC
Male	Top 10% difference	6.1019	10240.6388
	The rest 90%	2.0875	978.6246
	All proteins	2.4575	1774.7952
Female	Top 10% difference	5.8911	9771.7581
	The rest 90%	2.0725	867.6733
	All proteins	2.4520	1752.7179

5.2. Protein Essentiality. Essential proteins play a vital role in biological systems and are often termed lethal proteins because their absence can result in infertility or death [41]. Given the extensive research on identifying essential proteins, we compiled a list of those exhibiting significant differences in BNS for further analysis. The identification of essential proteins through network analysis involves various metrics, with validated measurements typically linked to DC, CC, and BC [42]. However, in our datasets, CC did not produce significant results that could serve as markers for essential proteins.

In addition to centrality measures, our findings on protein essentiality reveal that several proteins within the top 10% BNS differences are consistently expressed across all network datasets. By combining these insights, we identified several essential proteins related to aging for each gender that are considered crucial candidates for drug targeting, as listed below.

- Male essential aging proteins: P35222, Q9UKE5, Q12888, P25963, P32121, P19387, P09619, P13010, P36405, Q13625, P45983, Q16665, P04150, P06213, O14920, P20226, Q13616, P02786, P01112, O43318, P20936, and P60709.
- Female essential aging proteins: P35222, Q12888, P45983, P04150, P02786, P01112, P20936, P25963, P00533, Q16665, Q8TEW0, and Q13451.

The 28 important proteins discovered in the study had a high DC and BC, highlighting their importance in protein-protein interaction networks (PPINs). The central positions of these proteins in the network highlight their importance in ensuring network stability and functionality. From a mathematical standpoint, proteins with a high DC serve as hubs, connecting to multiple other proteins and playing an important role in the network's structural integrity [43]. Because of their high connection, they play an important role in network cohesiveness, and targeting these hubs can effectively alter overall network dynamics, which is especially useful in addressing the complex processes involved in aging.

Furthermore, the high betweenness centrality of these proteins suggests that they act as important connectors or bridges within the network. These proteins are engaged in many shortest pathways between other nodes, allowing for effective communication across network clusters [44]. Hence, targeting these bridge proteins makes it possible to influence the flow of information and regulatory signals within the network, potentially leading to broad and systemic therapeutic effects. This makes them very appealing candidates for drug targeting, as interventions at these locations might have far-reaching consequences for the network's behavior and stability [45].

Moreover, the essentiality of these 28 proteins in aging processes adds another layer of significance. In network theory, essential nodes are those whose removal causes major disruptions in network functionality. These proteins play important roles in essential biological processes that preserve cellular homeostasis and efficiency as humans age [46]. Targeting these critical

age-related proteins will increase the network's resilience to perturbations and general stability, potentially lessening the effects of aging and prolonging life duration [47].

Considering these proteins' critical roles and high centrality, modulating their activity may have a significant impact on network behavior. Therefore, improving the function of an essential protein that degrades with age can help mitigate the decline associated with aging and restore network efficiency. On the other hand, network dysfunction can be avoided by blocking a protein that becomes detrimental [48]. Since these high-centrality proteins are well-characterized, it is easier to create targeted interventions targeting these crucial nodes and reduce inadvertent network disruptions.

Previous examples from other fields, like epidemiology and telecommunications, show that targeting high-centrality nodes is beneficial for controlling the spread of information or illness [49]. Applying these principles to PPINs in the context of aging can result in beneficial therapeutic approaches. In conclusion, the 28 important proteins found, with their high degree and betweenness centrality, are computationally robust therapeutic targets due to their critical roles in network structure and dynamics. Targeting these proteins can have a large therapeutic effect, stabilizing and optimizing the network to battle the difficulties of aging.

6. CONCLUSION

In this study, the BNS proved effective in pinpointing proteins within aging PPINs. By examining centrality indicators like DC and BC, we pinpointed 28 proteins showing high differences in BNS values and consistent expression across multiple datasets. These results not only validate the utility of network analysis for identifying drug targets but also underscore the significance of key proteins in processes related to aging. Hence, this study explores the changes within aging networks by integrating essential characteristics.

However, this study points out some areas where more research is needed. Exploring filtration techniques could enhance the reliability of the findings by offering fresh perspectives on the importance of proteins. Additionally, contrasting homology outcomes with network analysis methods might enhance our comprehension of how network structure relates to biological functions in aging. Subsequent research should incorporate biological experiments to confirm the

significance of identified proteins, delve into their roles and interactions within aging processes, and assess their potential for therapeutic use in developing drugs for age-related conditions.

ACKNOWLEDGEMENT

The research is supported by research grant FRGS/1/2020/STG06/UKM/02/6.

CONFLICT OF INTERESTS

The authors declare that there is no conflict of interests.

REFERENCES

[1] P.D. Delmas, D. Stenner, H.W. Wahner, et al. Increase in serum bone gamma-carboxyglutamic acid protein with aging in women. Implications for the mechanism of age-related bone loss, J. Clin. Invest. 71 (1983), 1316–1321. https://doi.org/10.1172/jci110882.

[2] M.V. Narici, C.N. Maganaris, N.D. Reeves, P. Capodaglio, Effect of aging on human muscle architecture, J. Appl. Physiol. 95 (2003), 2229–2234. https://doi.org/10.1152/japplphysiol.00433.2003.

[3] G. Sharma, J. Goodwin, Effect of aging on respiratory system physiology and immunology, Clin. Intervent. Aging 1 (2006), 253–260. https://doi.org/10.2147/ciia.2006.1.3.253.

[4] M. Mather, L.L. Carstensen, Aging and motivated cognition: the positivity effect in attention and memory, Trends Cognit. Sci. 9 (2005), 496–502. https://doi.org/10.1016/j.tics.2005.08.005.

[5] M.C. Irizarry, M.E. Gurol, S. Raju, et al. Association of homocysteine with plasma amyloid β protein in aging and neurodegenerative disease, Neurology 65 (2005), 1402–1408. https://doi.org/10.1212/01.wnl.0000183063.99107.5c.

[6] F. Fabris, J.P. de Magalhaes, A.A. Freitas, A review of supervised machine learning applied to ageing research, Biogerontology 18 (2017), 171–188. https://doi.org/10.1007/s10522-017-9683-y.

[7] F.E. Faisal, T. Milenković, Dynamic networks reveal key players in aging, Bioinformatics 30 (2014), 1721–1729. https://doi.org/10.1093/bioinformatics/btu089.

[8] H. Syukor, A.B. Sakhinah, Characterization of essential protein in aging based on network analysis, J. Phys.: Conf. Ser. 1366 (2019), 012026. https://doi.org/10.1088/1742-6596/1366/1/012026.

[9] H. Yu, D. Greenbaum, H.X. Lu, et al. Genomic analysis of essentiality within protein networks, Trends Genetics 20 (2004), 227–231. https://doi.org/10.1016/j.tig.2004.04.008.

[10] H. Xu, J. Zhang, J. Yang, et al. Measurement of nodes importance for complex networks structural-holes-oriented, in: W. Che, Q. Han, H. Wang, et al. (Eds.), Social Computing, Springer Singapore, Singapore, 2016: pp. 458–469. https://doi.org/10.1007/978-981-10-2053-7_41.

[11] H. Xu, J. Zhang, J. Yang, L. Lun, Assessing nodes' importance in complex networks using structural holes, Int. J. High Perform. Comput. Network. 12 (2018), 314–323. https://doi.org/10.1504/IJHPCN.2018.094951.

[12] M. Syzdykbayev, H.A. Karimi, Persistent homology for detection of objects from mobile LiDAR point cloud data in autonomous vehicles, in: K. Arai, S. Kapoor (Eds.), Advances in Computer Vision, Springer, 2020: pp. 458–472. https://doi.org/10.1007/978-3-030-17798-0_37.

[13] A.N. Duman, Grain analysis of atomic force microscopy images via persistent homology, Ultramicroscopy 220 (2021), 113176. https://doi.org/10.1016/j.ultramic.2020.113176.

[14] N. Ravishanker, R. Chen, An introduction to persistent homology for time series, WIREs Comput. Stat. 13 (2021), e1548. https://doi.org/10.1002/wics.1548.

[15] M.E. Aktas, E. Akbas, A.E. Fatmaoui, Persistence homology of networks: methods and applications, Appl. Netw. Sci. 4 (2019), 61. https://doi.org/10.1007/s41109-019-0179-3.

[16] S. Chowdhury, F. Mémoli, A functorial dowker theorem and persistent homology of asymmetric networks, J Appl. Comput. Topol. 2 (2018), 115–175. https://doi.org/10.1007/s41468-018-0020-6.

[17] D. Horak, S. Maletić, M. Rajković, Persistent homology of complex networks, J. Stat. Mech. 2009 (2009), P03034. https://doi.org/10.1088/1742-5468/2009/03/P03034.

[18] G. Carlsson, V. De Silva, Zigzag persistence, Found. Comput. Math. 10 (2010), 367–405. https://doi.org/10.1007/s10208-010-9066-0.

[19] S. Pal, T.J. Moore, R. Ramanathan, A. Swami, Comparative topological signatures of growing collaboration networks, in: B. Gonçalves, R. Menezes, R. Sinatra, V. Zlatic (Eds.), Complex Networks VIII, Springer International Publishing, Cham, 2017: pp. 201–209. https://doi.org/10.1007/978-3-319-54241-6_18.

[20] W. Huang, A. Ribeiro, Persistent homology lower bounds on high-order network distances, IEEE Trans. Signal Process. 65 (2017), 319–334. https://doi.org/10.1109/TSP.2016.2620963.

[21] S. Benzekry, J.A. Tuszynski, E.A. Rietman, G. Lakka Klement, Design principles for cancer therapy guided by changes in complexity of protein-protein interaction networks, Biol. Direct 10 (2015), 32. https://doi.org/10.1186/s13062-015-0058-5.

[22] B. Rieck, U. Fugacci, J. Lukasczyk, H. Leitte, Clique community persistence: a topological visual analysis approach for complex networks, IEEE Trans. Visual. Computer Graph. 24 (2018), 822–831. https://doi.org/10.1109/TVCG.2017.2744321.

[23] M.K. Chung, J.L. Hanson, H. Lee, et al. Persistent homological sparse network approach to detecting white matter abnormality in maltreated children: mri and dti multimodal study, in: C. Salinesi, M.C. Norrie, Ó. Pastor (Eds.), Advanced Information Systems Engineering, Springer Berlin Heidelberg, Berlin, Heidelberg, 2013: pp. 300–307. https://doi.org/10.1007/978-3-642-40811-3_38.

[24] C. Giusti, R. Ghrist, D.S. Bassett, Two's company, three (or more) is a simplex: algebraic-topological tools for understanding higher-order structure in neural data, J. Comput. Neurosci. 41 (2016), 1–14. https://doi.org/10.1007/s10827-016-0608-6.

[25] P.S.P. Ignacio, I.K. Darcy, Tracing patterns and shapes in remittance and migration networks via persistent homology, EPJ Data Sci. 8 (2019), 1. https://doi.org/10.1140/epjds/s13688-018-0179-z.

[26] A. Khalid, B.S. Kim, M.K. Chung, et al. Tracing the evolution of multi-scale functional networks in a mouse model of depression using persistent brain network homology, NeuroImage 101 (2014), 351–363. https://doi.org/10.1016/j.neuroimage.2014.07.040.

[27] M. Rucco, F. Castiglione, E. Merelli, M. Pettini, Characterisation of the idiotypic immune network through persistent entropy, in: S. Battiston, F. De Pellegrini, G. Caldarelli, E. Merelli (Eds.), Proceedings of ECCS 2014, Springer International Publishing, Cham, 2016: pp. 117–128. https://doi.org/10.1007/978-3-319-29228-1_11.

[28] A. Sizemore, C. Giusti, D.S. Bassett, Classification of weighted networks through mesoscale homological features, J. Complex Netw. 5 (2016), 245–273. https://doi.org/10.1093/comnet/cnw013.

[29] A. Suh, M. Hajij, B. Wang, C. Scheidegger, P. Rosen, Persistent homology guided force-directed graph layouts, IEEE Trans. Visual. Computer Graph. 26 (2020), 697–707. https://doi.org/10.1109/TVCG.2019.2934802.

[30] N.C. Berchtold, D.H. Cribbs, P.D. Coleman, J. Rogers, E. Head, R. Kim, T. Beach, C. Miller, J. Troncoso, J.Q. Trojanowski, H.R. Zielke, C.W. Cotman, Gene expression changes in the course of normal brain aging are sexually dimorphic, Proceedings of the National Academy of Sciences 105 (2008), 15605–15610. https://doi.org/10.1073/pnas.0806883105.

[31] L. Salwinski, C.S. Miller, A.J. Smith, et al. The database of interacting proteins: 2004 update, Nucleic Acids Res. 32 (2004), 449D – 451. https://doi.org/10.1093/nar/gkh086.

[32] T.M. Witten, D. Bonchev, Predicting aging/longevity-related genes in the nematode caenorhabditis elegans, Chem. Biodivers. 4 (2007), 2639–2655. https://doi.org/10.1002/cbdv.200790216.

[33] F. Fouss, A. Pirotte, J. Renders, M. Saerens, Random-walk computation of similarities between nodes of a graph with application to collaborative recommendation, IEEE Trans. Knowl. Data Eng. 19 (2007), 355–369. https://doi.org/10.1109/TKDE.2007.46.

[34] Y. Lipman, R.M. Rustamov, T.A. Funkhouser, Biharmonic distance, ACM Trans. Graph. 29 (2010), 1–11. https://doi.org/10.1145/1805964.1805971.

[35] M. Hajij, B. Wang, C. Scheidegger, P. Rosen, Visual detection of structural changes in time-varying graphs using persistent homology, in: 2018 IEEE Pacific Visualization Symposium (PacificVis), IEEE, Kobe, 2018: pp. 125–134. https://doi.org/10.1109/PacificVis.2018.00024.

[36] R. Agarwal, M. Caesar, P.B. Godfrey, B.Y. Zhao, Shortest paths in less than a millisecond, in: Proceedings of the 2012 ACM Workshop on Workshop on Online Social Networks, ACM, Helsinki Finland, 2012: pp. 37–42. https://doi.org/10.1145/2342549.2342559.

[37] C. Tóth, J. O'Rourke, J.E. Goodman, eds., Handbook of discrete and computational geometry, CRC Press, Boca Raton, 2017.

[38] U. Islambekov, Y.R. Gel, Unsupervised space–time clustering using persistent homology, Environmetrics 30 (2019), e2539. https://doi.org/10.1002/env.2539.

[39] L.C. Freeman, A set of measures of centrality based on betweenness, Sociometry 40 (1977), 35–41. https://doi.org/10.2307/3033543.

[40] U. Brandes, A faster algorithm for betweenness centrality, J. Math. Sociol. 25 (2001), 163–177. https://doi.org/10.1080/0022250X.2001.9990249.

[41] W. Peng, J. Wang, W. Wang, Q. Liu, F.-X. Wu, Y. Pan, Iteration method for predicting essential proteins based on orthology and protein-protein interaction networks, BMC Syst. Biol. 6 (2012), 87. https://doi.org/10.1186/1752-0509-6-87.

[42] S. Rasti, C. Vogiatzis, A survey of computational methods in protein–protein interaction networks, Ann. Oper. Res. 276 (2019), 35–87. https://doi.org/10.1007/s10479-018-2956-2.

[43] N. Singh, S. Rai, R. Bhatnagar, S. Bhatnagar, Network analysis of host-pathogen protein interactions in microbe induced cardiovascular diseases, In Silico Biol. 14 (2022), 115–133. https://doi.org/10.3233/ISB-210238.

[44] E. Estrada, D.J. Higham, N. Hatano, Communicability betweenness in complex networks, Physica A: Statistical Mechanics and Its Applications 388 (2009), 764–774. https://doi.org/10.1016/j.physa.2008.11.011.

[45] K. McGarry, S. McDonald, Complex network theory for the identification and assessment of candidate protein targets, Computers Biol. Med. 97 (2018), 113–123. https://doi.org/10.1016/j.compbiomed.2018.04.015.

[46] C.C. Lin, H.F. Juan, J.T. Hsiang, et al. Essential core of protein-protein interaction network in escherichia coli, Journal of Proteome Research 8 (2009), 1925–1931. https://doi.org/10.1021/pr8008786.

[47] F.A. Rodrigues, L.D.F. Costa, A.L. Barbieri, Resilience of protein–protein interaction networks as determined by their large-scale topological features, Mol. BioSyst. 7 (2011), 1263. https://doi.org/10.1039/c0mb00256a.

[48] C. Liang, J. Luo, D. Song, Network simulation reveals significant contribution of network motifs to the age-dependency of yeast protein–protein interaction networks, Mol. BioSyst. 10 (2014), 2277. https://doi.org/10.1039/C4MB00230J.

[49] H. Ushijima-Mwesigwa, Z. Khan, M.A. Chowdhury, I. Safro, Centralities for networks with consumable resources, Netw. Sci. 7 (2019), 376–401. https://doi.org/10.1017/nws.2019.7.